Sensor data processing preprint

Quantum Approach to Satellite Image Data Compression and Analysis

Sathwik Reddy Majji, Avinash Chalumuri, and B. S. Manoj
Indian Institute of Space Science and Technology, Thiruvananthapuram 695547, India

Manuscript received Month DD, Year; revised Month DD, Year; accepted Month DD, Year. Date of publication Month DD, Year.

Abstract—Due to the rapid development of satellite imaging sensors, high-resolution images are being generated for use. Various image processing algorithms, such as deep learning models, require images of reduced sizes given the computational constraints. Hence, preprocessing the images to reduce their size is crucial for any deep learning model. This paper proposes a novel approach to compress satellite images using quantum computing. A comparative study on different standard data embedding techniques used in quantum computing is undertaken. We propose four quantum compression techniques (QCTs) by extending the unitary operations of amplitude encoding for compressing satellite images. The proposed methods provide exponential scaling as amplitude encoding is used, where 2^n classical data values are encoded into n qubits. Compression performance, visual evaluation, and quality metric evaluation were carried out to assess the proposed compression techniques. Our experimental results showed that the crucial patterns in images are retained in the compressed images without quality loss even after 75% compression. The compressed images can be used for post-processing tasks such as classification using classical or quantum computing algorithms.

Index Terms—Quantum computing, data encoding, data compression, satellite image processing, quantum circuit, image size reduction.

I. INTRODUCTION

Imaging sensors of remote sensing satellites generate a large amount of data which is used for various real-time applications such as classification and object detection [1]. However, extensive storage and computational facilities are required to store and process high-resolution satellite images. Hence, traditional computational methods are sometimes insufficient. Quantum computing [2] is a rapidly growing technology based on quantum-mechanical properties for computation. Classical computers can only encode data in bits that take a value of either 0 or 1. Whereas quantum computers encode data in more than two states at a time using quantum-mechanical properties such as superposition and entanglement. Thus, quantum computers are fundamentally different in processing information than classical computers.

A quantum bit or qubit is the basic unit of information in quantum computing. A qubit differs from a classical bit as qubits can be represented using a superposition of two basis states, $|0\rangle$ and $|1\rangle$. Hence, a qubit is a two-dimensional quantum system and similarly d-dimensional quantum systems (qudits) can be represented using superposition of d basis states such as $|0\rangle, |1\rangle, |2\rangle, \ldots, |d\rangle$.

As discussed earlier, analyzing remotely sensed images requires storing and processing massive data. Also, training deep learning models with large images increases the complexity of handling the training phase [3]. Quantum computing can solve the problem as quantum computers efficiently handle vast amounts of data by providing exponential scaling using qubits for computation [4].

This letter introduces a novel image data compression approach using quantum computing where image data in the classical domain is encoded into a quantum computer for compression. The compressed image data in the quantum domain is later transformed into a down-scaled image in the classical domain for desired post-processing tasks. The main contributions of this work are as follows.

1) We compared three existing quantum encoding techniques from the perspective of satellite imagery.
2) We propose four quantum embedding methods using quantum circuits for high-resolution satellite image compression.
3) We experimented with the four methods on a dataset comprising 200 satellite images to reduce the size of the images.
4) We analyzed the effect of tuning the quantum circuits on the compressed image data using performance, visual and objective evaluation methods.

The rest of this letter is organized as follows. Section II discusses the details of the dataset used in this work and a comparative study of the standard data encoding techniques. In Section III, we propose four data compression techniques using quantum circuits. Section IV provides the details of the experiments carried out using the proposed technique along with results and discussion. In the end, conclusions are drawn in Section V.

II. DATASET AND DATA ENCODING TECHNIQUES

In this work, we used a dataset of 200 satellite image tiles from [5] with less than 1% cloud coverage for the experiments. The chosen dataset has 100 pairs of SAR (grayscale) and Optical (RGB) images of the same area and taken at the same time. The 100 image pairs are split into two classes (50 image pairs each of airports and forestry). The selected satellite image tiles have a tile size of 1024×1024 pixels and a tile area of around $105km^2$.

Data encoding is essential in processing information using qubits on a quantum computer. The way of data encoding affects the efficiency of computational algorithms [6]. However, selecting a specific data encoding mechanism for high-resolution satellite images is an interesting research area. The properties of the data and the nature of the target remote sensing application are to be considered while selecting data encoding algorithms. The huge size of images is another consideration when selecting such a data encoding mechanism. Encoding image pixel data is the primary step in processing high-

Corresponding author: B. S. Manoj (e-mail: bsmanoj@ieee.org).
Associate Editor: NAME.
Digital Object Identifier URL

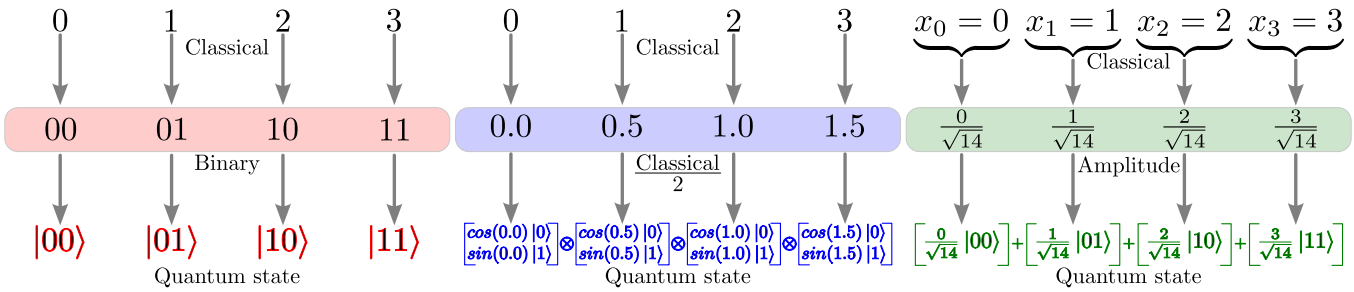

(a) Basis embedding (b) Angle embedding (c) Amplitude embedding

Fig. 1: Data encoding using the three standard qubit embedding techniques.

resolution satellite images. Embedding methods for data encoding are based on the following three standard techniques.

1) ***Basis Embedding****:* In basis embedding [6], the classical data is converted to binary form, then the string of binary inputs is translated as a quantum basis state as shown in Figure 1a. The binary value of classical data is encoded as a basis state with an amplitude of one. A classical data value with n binary bits is encoded using a basis state of n qubits in basis embedding. Thus, basis embedding requires many qubits to encode high-dimensional data because binary representations of the classical data are encoded as basis states.

2) ***Angle Embedding****:* In angle embedding, classical data features are encoded as the rotational angles of qubits using unitary operations as shown in Figure 1b. The qubit rotation can be achieved around x-axis $R_x(v^i)$ or y-axis $R_y(v^i)$ or z-axis $R_z(v^i)$ in a Bloch sphere [7] where v^i is the classical data value. The angle embedding encodes n classical features into a minimum of n qubits [6] where each feature is encoded as a rotational angle of a quantum rotational gate.

3) ***Amplitude Embedding****:* In amplitude embedding, the classical features are mapped into amplitudes of a quantum state. The initial step in amplitude embedding is converting classical data into angular representations, as shown in Figure 1c. The data is encoded into amplitudes of quantum states using uniformly controlled rotations [8] as per Equation 1.

$$\left|\psi_{amp}\right\rangle = R\left(x_i, \beta\right)\left|k_1 k_2, ..., k_{s-2} k_{s-1}\right\rangle \left|k_s\right\rangle \tag{1}$$

R is a function of x_i and β, where x_i is the i^{th} classical feature vector and β is a parameter depending on the dimensions of the classical features [6]. State $\left|\psi_{amp}\right\rangle$ is the result of n rotations on y-axis in a cascade where n is the power for embedding a classical feature vector x_i. In general, to associate each amplitude with a component of the input vector, the dimension of the vector must be equal to a power of two because the vector space of an n qubit register has dimension 2^n. After the rotations, the input vector $X = \{x_1, x_2, \ldots, x_n\}$ is encoded in the amplitudes of the quantum state as

$$|\psi\rangle = \sum_{i=0}^{n-1} x_i \,|i\rangle \tag{2}$$

where, x_i is the normalized value of the i^{th} classical feature.

A. Selection of Embedding Technique

Basis embedding is a primary way of encoding classical data using basis states. However, basis embedding encodes binary features into basis states; hence, the dimensionality and qubits requirement increases drastically. In angle embedding, a minimum of n qubits to encode n classical features. At present, noisy intermediate-scale quantum devices (NISQs) contain limited qubits to work with, and also maintaining the coherence of many qubits is a difficult task [9]. Hence, basis and angle embedding schemes are not the best choices for satellite images as encoding the classical data require many qubits. In amplitude embedding, 2^n classical data features can be encoded using only n qubits. Since exponentially fewer qubits are required compared to other standard encoding techniques for data encoding, amplitude embedding is more suitable for satellite image data compression.

In this work, we opted for a flexible approach where amplitude embedding followed by unitary operations are used as the quantum embedding method to encode and process satellite imagery. The unitary gates are meant for fine tuning the results.

III. QUANTUM CIRCUITS FOR DATA COMPRESSION

This section discusses the four proposed quantum compression techniques (QCTs) using amplitude embedding scheme followed by unitary operations to process and compress the remotely sensed image data. All four proposed compression techniques work on a 4-wired quantum circuit that needs encoding of $2^4 = 16$ classical input parameters. The details of each QCT are provided as follows.

1) ***QCT_1****:* In this compression technique, classical image pixel features (p) are encoded onto the 4–Wired quantum embedding circuit (QEC) using an amplitude embedding scheme (U_{amp}) with $|0\rangle$ as the initial state of all four qubits [10]. After encoding all the classical features into four qubits, *Pauli-Z* measurement operator is used to measure the qubit values (q) as shown in Figure 2.

2) ***QCT_2****:* In this technique, encoding classical features (p) through U_{amp}, is similar to QCT_1, but has *Pauli-X* operation at each wire after encoding step as shown in Figure 2. The four wires after the *Pauli-X* operation are measured using *Pauli-Z* measurement operator.

3) ***QCT_3****:* This technique starts in the same way as QCT_1 by encoding classical data p through U_{amp}. After the data encoding step, the information in the four wires is entangled with the help of three *CNOT* operations, as shown in Figure 2. The four entangled wires are then measured using *Pauli-Z* measurement operator.

4) ***QCT_4****:* This compression technique is a combination of QCT_1, QCT_2 and QCT_3 where the classical image pixel data (p) is encoded through U_{amp}. After encoding the data, each wire is subjected to *Pauli-X* operation, and the resulting qubits are then entangled with three *CNOT* operations as shown in Figure 2. The four entangled qubits are then measured using *Pauli-Z* measurement operator.

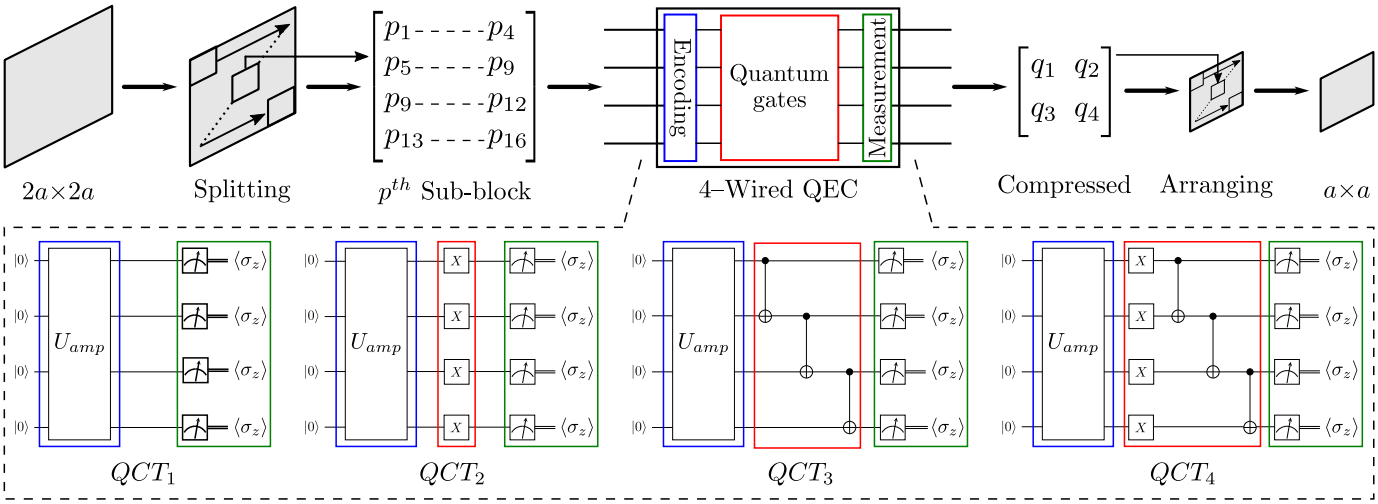

Fig. 2: Schematic diagram of the steps involved in high-resolution image processing.

IV. EXPERIMENTS AND RESULTS

The experiments are conducted using *PennyLane* [11] Python module. The chosen 200 SAR and optical images are downsized from 1024×1024 to 400×400 due to the current limitation in the availability of quantum computational resources. First, each downsized image is split into sub-blocks containing 16-pixel data values, as shown in Figure 2. The initial state of all qubits is set to $|0\rangle$ by default and the pixel values in each sub-block ($p_1, p_2, \ldots, p_{16}$) are then encoded into a 4–Wired QEC by (U_{amp}) embedding scheme [10]. Later, a set of post-encoding quantum gates further modify the classical encoded data in the quantum domain. Finally, the modified quantum data is measured and converted back to the classical domain with *Pauli-Z* measurement operator at the end of each wire. Since the work is with four wires, four measured values (q_1, q_2, q_3, and q_4) are obtained in the classical domain with each value between [-1, 1]. The measured values are scaled to [0, 255] for further processing. The resulting sub-block is arranged to recreate a compressed image of 200×200 as shown in Figure 2. Hence, this method theoretically compresses a sub-block of 16 values to 4 values, resulting in 75% compression.

The effect of quantum gates in overall image compression can be studied with the four proposed techniques (QCT_1, QCT_2, QCT_3, and QCT_4). For this study, the compressed images are evaluated by three methods. The first is to analyze the four techniques based on their compression performance with the image dataset. The second is a visual analysis of the four techniques, which is a direct and commonly used evaluation approach. Since evaluating compressed images on visual interpretation is subjective, we have proceeded with the final evaluation method where the compressed images of all four techniques are objectively assessed with well-established quality metrics. The three evaluation methods to evaluate the proposed techniques are discussed as follows.

A. Compression Performance

As noted in the above section, the theoretical data compression rate of the proposed four techniques is (16 pixels)/(4 values) = 4 : 1. However, a comparison with an actual image dataset is required for analyzing the four compression techniques. Hence the average compression rates of the four techniques with SAR and optical image datasets are provided in Table 1. It is observed that the actual compression rates of the four proposed techniques are near to the theoretical value of 4 : 1. Also, all four techniques show a better compression rate with SAR images when compared to optical images. This could be due to the technique dealing with three bands (RGB) in the case of optical images in comparison with only one grayscale band in SAR imagery. Even though the overall compression rates of all the four techniques are near to 4 : 1, comparing the compression rates of QCT_2 with QCT_1 and QCT_4 with QCT_3, it can be observed that the *Pauli-X* operation is impacting negatively in data compression performance. Another observation is that QCT_3 and QCT_4 compress better than the other two techniques implying that the entanglement of qubits through *CNOT* operation is improving the compression rates.

Table 1: Compression performance of the proposed techniques.

Input data size (MB)	Compression technique	Output data size (MB)	Compression ratio (In/Out)
100 optical images with total size = 38.0502	QCT_1	10.7545	3.53807 : 1
	QCT_2	10.7545	3.53807 : 1
	QCT_3	10.6226	3.58200 : 1
	QCT_4	10.6590	3.56977 : 1
100 SAR images with total size = 13.3040	QCT_1	3.44506	3.86176 : 1
	QCT_2	3.44510	3.86171 : 1
	QCT_3	3.34790	3.97383 : 1
	QCT_4	3.36338	3.95554 : 1

B. Visual Evaluation

Figure 3 shows eight sample SAR and optical image pairs in two dataset classes, along with the compressed images through each technique. Identifiable patterns are visible in all the compressed images. The compression of SAR imagery leads to distinguishable artificial structures such as airport runways, taxiways, paths, and constructions. In contrast, compression of optical imagery leads to better patterns in natural formations such as fields around airports, terrain structures, water bodies, etc. Therefore, a fusion of these two compressed image pairs, as proposed in [12] would further enhance the image. Also, images from QCT_1 and QCT_2 show better patterns when compared to images from the other two techniques.

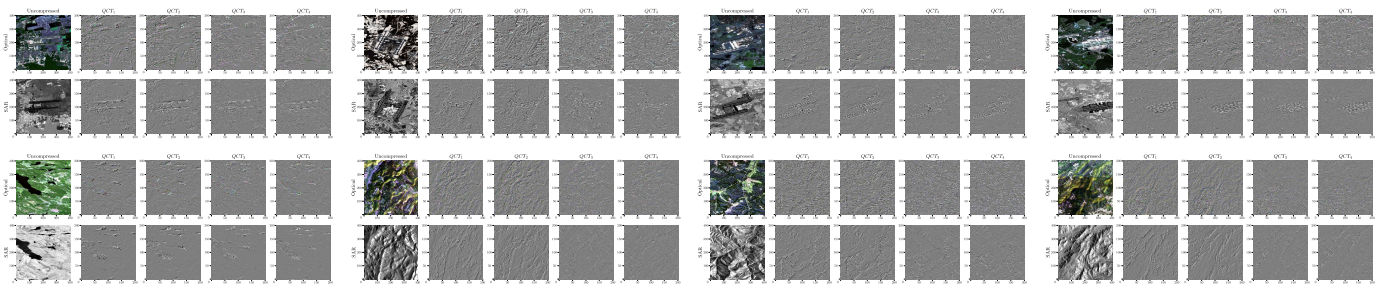

Fig. 3: Objective evaluation of eight selected SAR-Optical pairs and their compressed images.

Table 2: Objective evaluation of the compressed images with different quality metrics (each provided value is the average of 200 images).

Images	Technique	*RV*	*PSNR*	*SSIM*	*UIQI*
100 optical images	QCT_1	0.64595	17.6239	0.97959	0.67290
	QCT_2	0.64595	16.1442	0.97878	0.64452
	QCT_3	0.69528	16.9517	0.97870	0.66253
	QCT_4	0.69532	16.3907	0.97826	0.64825
100 SAR images	QCT_1	0.77409	17.3483	0.98976	0.84298
	QCT_2	0.77409	15.4930	0.98913	0.82017
	QCT_3	0.82938	16.7122	0.98943	0.83669
	QCT_4	0.82939	16.0712	0.98911	0.82641

C. Objective Evaluation

In this work, four benchmark quality metrics are used for the objective evaluation of the compressed images. They are Relative Variance (*RV*) [12], Peak Signal-to-Noise Ratio (*PSNR*) [13], Structural Similarity Index Measure (*SSIM*) [12], and Universal Image Quality Index (*UIQI*) [14]. From Table 2, it is observed that the *RV* and *PSNR* values of compressed optical images are generally better than those of compressed SAR images implying a lower noise in compressed optical images. However, all *SSIM* and *UIQI* values of compressed SAR images are better than those of compressed optical images. This indicates that though the compressed SAR images contain noise, they are structurally more similar and have greater quality than the compressed optical images. Comparing the *RV* values of QCT_1 and QCT_2 or QCT_3 and QCT_4 show that the *Pauli-X* operation as a post encoding operation make a little to no change in details of (or patterns in) images. However, comparing the *PSNR*, *SSIM*, and *UIQI* values of QCT_1 and QCT_2 shows that the *Pauli-X* operation alters the pixel intensity values of the compressed images. Another observation is that QCT_1 and QCT_3, in general, perform better than the other two techniques implying that post-encoding entanglement of qubits is preferable over rotational quantum operations.

V. CONCLUSIONS AND FUTURE WORK

In summary, we introduced a novel approach to compressing image data using quantum computing. Based on this approach, four quantum compression techniques (QCTs) were proposed and were applied to compress a dataset of remotely sensed 200 SAR and optical images. Visual and quality metric evaluations were carried out to assess the compressed images. The results showed that the proposed techniques performed well at compression and were on par with the calculated theoretical value of compression. Also, the crucial patterns in images are retained in the compressed images without significant loss of quality even at 75% compression.

The current limitation in the availability of qubits in real hardware has forced the use of four-qubit quantum circuits in all QCTs. Use of different quantum circuits is possible with the development and availability of additional hardware resources. The experiments are limited to the use of a few sets of quantum gates, as this work focused on introducing the possibility of quantum techniques for image compression. Further tuning in quantum circuits can be achieved to enhance image compression and quality. As an extension of this work, classical or quantum post-processing algorithms can be designed to process the compressed images for remote sensing applications. Also, deep learning models can be trained with the compressed images for scene classification.

REFERENCES

[1] X. Zhang, L. Han, L. Han, and L. Zhu, "How well do deep learning-based methods for land cover classification and object detection perform on high resolution remote sensing imagery?" *Remote Sensing*, vol. 12, no. 3, p. 417, Jan. 2020.

[2] A. Steane, "Quantum computing," *Reports on Progress in Physics*, vol. 61, no. 2, p. 117, Feb. 1998.

[3] K. Simonyan and A. Zisserman, "Very deep convolutional networks for large-scale image recognition," *arXiv preprint arXiv:1409.1556*, Sep. 2014.

[4] B. M. Terhal, "Quantum supremacy, here we come," *Nature Physics*, vol. 14, no. 6, pp. 530–531, Jun. 2018.

[5] S. R. Majji, A. Chalumuri, R. Kune, and B. S. Manoj, "Data acquisition and utilization of quantum processed sar and optical images for scene classification," *IEEE TechRxiv Preprint*, May 2022.

[6] M. Schuld and F. Petruccione, *Supervised learning with quantum computers*. Springer, Aug. 2018, vol. 17.

[7] O. Gamel, "Entangled bloch spheres: Bloch matrix and two-qubit state space," *Physical Review A*, vol. 93, no. 6, p. 062320, Jun. 2016.

[8] M. Möttönen, J. J. Vartiainen, V. Bergholm, and M. M. Salomaa, "Transformation of quantum states using uniformly controlled rotations," *Quantum Info. Comput.*, vol. 5, no. 6, p. 467–473, Jun. 2005.

[9] J. Preskill, "Quantum Computing in the NISQ era and beyond," *Quantum*, vol. 2, p. 79, Aug. 2018.

[10] "qml.amplitudeembedding — pennylane 0.25.1 documentation," https://docs.pennylane.ai/en/stable/code/api/pennylane.AmplitudeEmbedding.html, (Accessed on 08/22/2022).

[11] V. Bergholm, J. Izaac, M. Schuld, C. Gogolin, and N. Killoran, "Pennylane: Automatic differentiation of hybrid quantum-classical computations," *arXiv preprint arXiv:1811.04968*, Nov. 2018.

[12] S. R. Majji, A. Chalumuri, R. Kune, and B. S. Manoj, "Quantum processing in fusion of sar and optical images for deep learning: A data-centric approach," *IEEE Access*, vol. 10, pp. 73 743–73 757, Jul. 2022.

[13] A. Horé and D. Ziou, "Image quality metrics: Psnr vs. ssim," in *2010 20th International Conference on Pattern Recognition*, Aug. 2010, pp. 2366–2369.

[14] Z. Wang and A. Bovik, "A universal image quality index," *IEEE Signal Processing Letters*, vol. 9, no. 3, pp. 81–84, Mar. 2002.